Supplementary material for:
Predicting gas record alteration in very low accumulation ice cores

Kévin Fourteau[1], Patricia Martinerie[1], Xavier Faïn[1], Alexey A. Ekaykin[2], Jérôme Chappellaz[1], and Vladimir Lipenkov[2]

[1]Univ. Grenoble Alpes, CNRS, IRD, Grenoble INP, IGE, F-38000 Grenoble, France

[2]Climate and Environmental Research Laboratory, Arctic and Antarctic Research Institute, St. Petersburg, 199397, Russia

Correspondence to: kevin.fourteau@univ-grenoble-alpes.fr or patricia.martinerie@univ-grenoble-alpes.fr

S1 NEEM atmospheric reference without deconvolution

In the main article, we used as atmospheric reference for the DO21 period the methane CFA data of Chappellaz et al. (2013) after a deconvolution. This was done as using the data without deconvolution leads to an inconsistency between the atmospheric reference and the Vostok record. Indeed, as illustrated in Figure S1 it is not possible to find a single gas age distribution that leads to adequate smoothing in the Vostok record. As it is unlikely that the gas age distribution of the enclosed gases changed in the Vostok record between the two methane increases of the DO21, we attribute this discrepancy to the fact the raw NEEM data cannot be used as atmospheric reference without deconvolution.

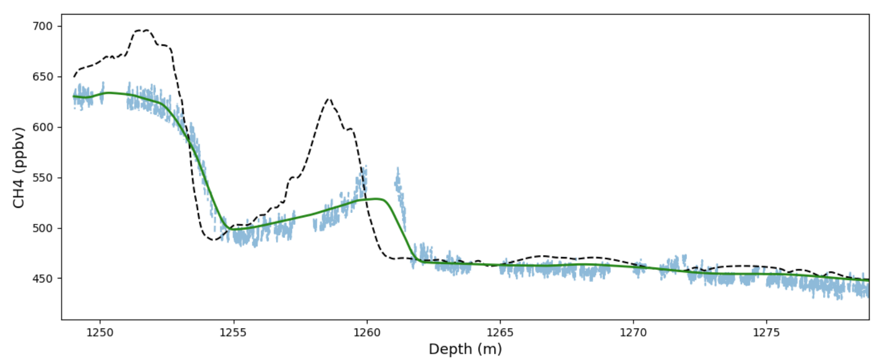

Figure S1. Illustration of the impossibility to find a gas age distribution that smooths the atmospheric scenario (in dashed black, NEEM data without deconvolution) in order to match the Vostok CFA measurements (in light blue). The smoothed version in green underestimates the fast event measured in the ice core around the 1260m depth.

S2 Zoom over layering artifacts

A closer look at the layering artifacts of the EDC96 DO6-9 section is shown in Figure S2. This highlights the structure of the layering artifacts, and their widths of a couple of centimeters. They are similar to the artifacts reported in Figure 1 if Fourteau et al. (2017).

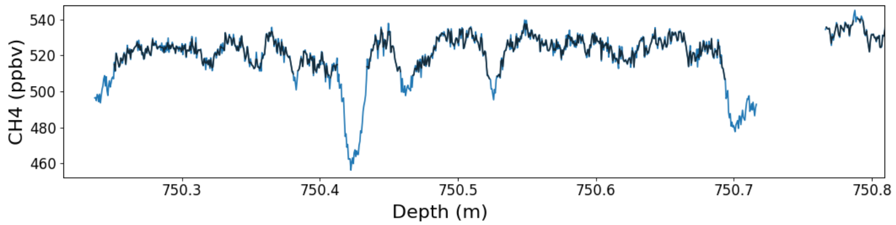

Figure S2. Zoom over the EDC96 DO6-9 methane record. The blue data are the raw CFA measurements. In black are the data cleaned for layering artifacts.

S3 Comparison of discrete and continuous methane data over the DO8

In this section we compare the discrete (Loulergue et al., 2008) and continuous (this study) methane measurements over the DO8 event in the EPICA Dome C record. Fourteau et al. (2017) pointed out that one the of the data point of Loulergue et al. (2008) might corresponds to an early closure artifact and is therefore not climatically relevant variability. This data point is highlighted with a blue circle in Figure S3. The high-resolution measurements confirm that this data point corresponds to an early closure artifact, the sample selected by Loulergue et al. (2008) being in a zone with a lot layering artifacts with similar methane concentration.

S4 Layering artifacts model, without impurity effect

In the main text, a parametrization was included to account for the enhancement of layering due to the presence of high calcium concentrations and variabilities. Here we present the result of the layering model for the DO6 to 9 period in the EDC96 ice core, without taking into account the enhancement due to chemistry. The output of the model is displayed in Figure S4. As seen on the figure, the model does not predict enough layering artifacts on the onset of the DO7 and 8. This highlights the necessity to take into account the effect of impurities on layering.

S5 Uncertainty on Gas Age Distributions

The extraction method yields an optimal GAD that minimizes the RMSD between the CFA measurements and the smoothed atmospheric reference. To quantify the uncertainties associated with the calculated GADs, we performed a dedicated analysis. For each of the five ice core sections, we studied the impact of choosing slightly modified location and scale parameters.
Practically, we modify the scale and location parameters until the resulting RMSD is 15% larger than its optimal value. The

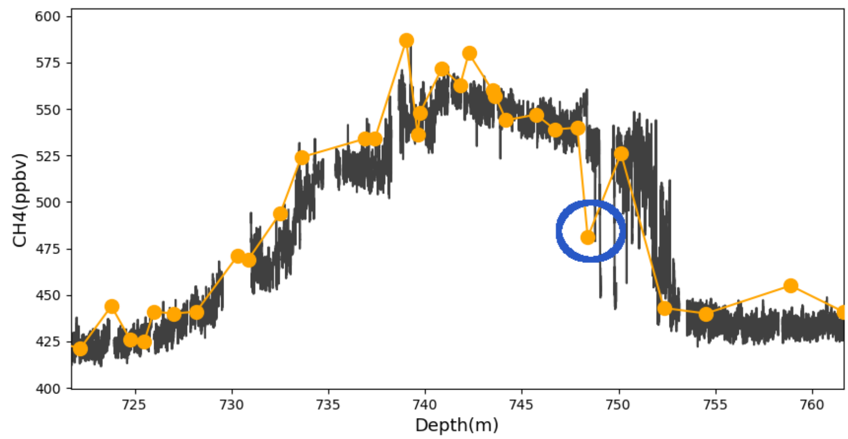

Figure S3. In orange: discrete methane measurements of the DO8 event in the EPICA Dome C record (Loulergue et al., 2008). In black: continuous methane measurements of the same event in the EPICA Dome C record (this study). In blue we highlight a data point of the discrete record corresponding to an early closure artifact.

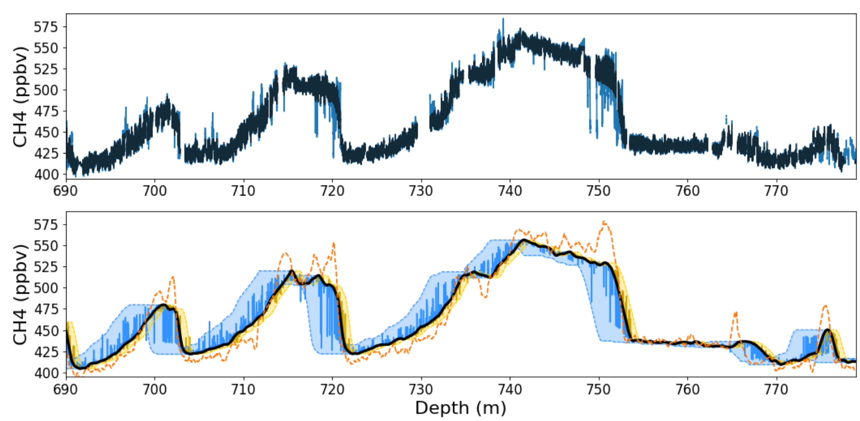

Figure S4. Results of the layering model. This figure is similar to Figure 5 of the main article, but does not include the effect of impurity driven enhancement of layering.

location and scales were modified following straight lines in the {location, scale} space, starting from the optimal values (Figure S5). We then obtained a set of 10 GADs meant to represent the limit of acceptable distributions. These GADs and their corresponding smoothed methane records in the ice are displayed in Figures S6 to S10. In the right panel of these figures, we also represented the set of location and scale values that increase the RMSD by 15%. The regions enclosed by the those values can be viewed as the uncertainty ranges of the location and scale parameters.

To better appreciate the uncertainty associates with the EDC96 and Vostok glacial GADs, we plotted their uncertainty ranges on the common Figure S11. It confirms that the EDC96 age distribution is less well constrained than Vostok GAD.

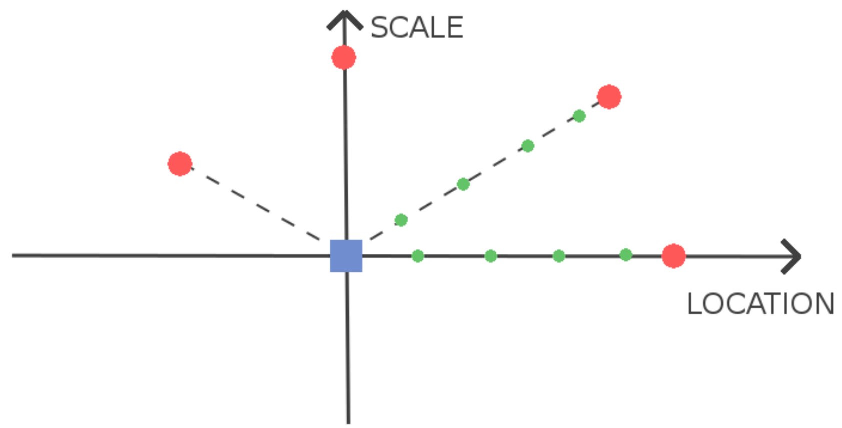

Figure S5. Method used to modify the location and scale parameters for the uncertainty assessment. Starting from the optimal values (blue square), the location and scale parameters are moved away following straight lines (dashed lines). If the new RMSD differs by less than 15% with the optimal value (green dots) the location and scale are further modified, until the 15% are reached (red dots). Then the parameters are modified following a new line. In total 10 different lines are tested.

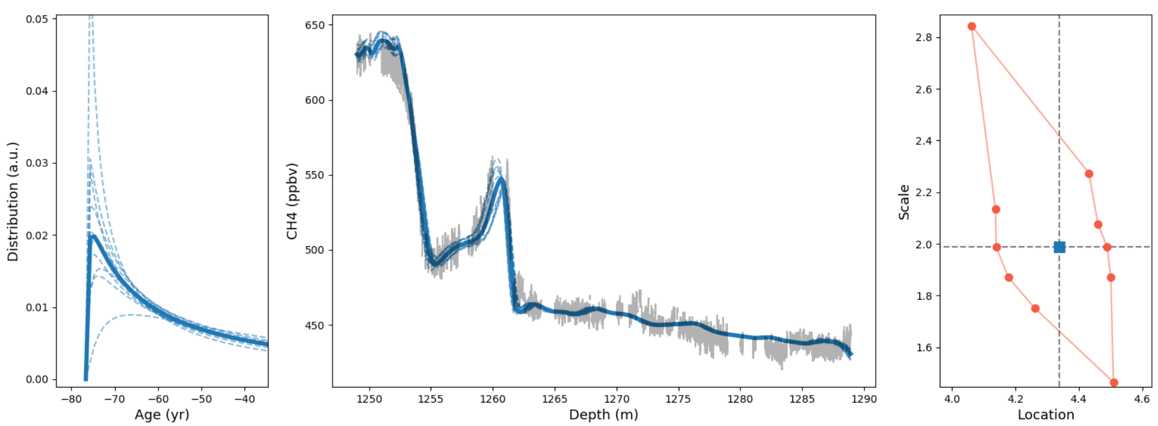

Figure S6. GAD for the DO21 event in Vostok. Left panel: Optimal gas age distribution as a bold solid line. Age distributions resulting in 15% RMSD increases are shown as dashed lines. Middle panel: Methane smoothed record using the optimal GAD as a bold solid line, and methane smoothed records using the 15% higher RMSD distributions are displayed as dashed lines. CFA measurements are displayed in gray. Right panel: Location and scale parameters defining the gas age distributions. The blue square marks the optimal parameters and the red dots represent age distributions resulting in a 15% increase of RMSD.

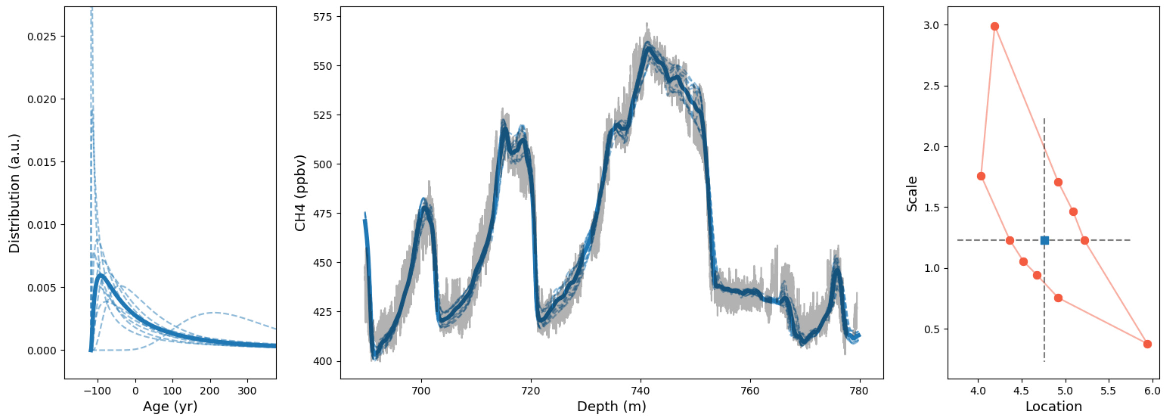

Figure S7. Same as Figure S3 for DO6-8 events in EDC96.

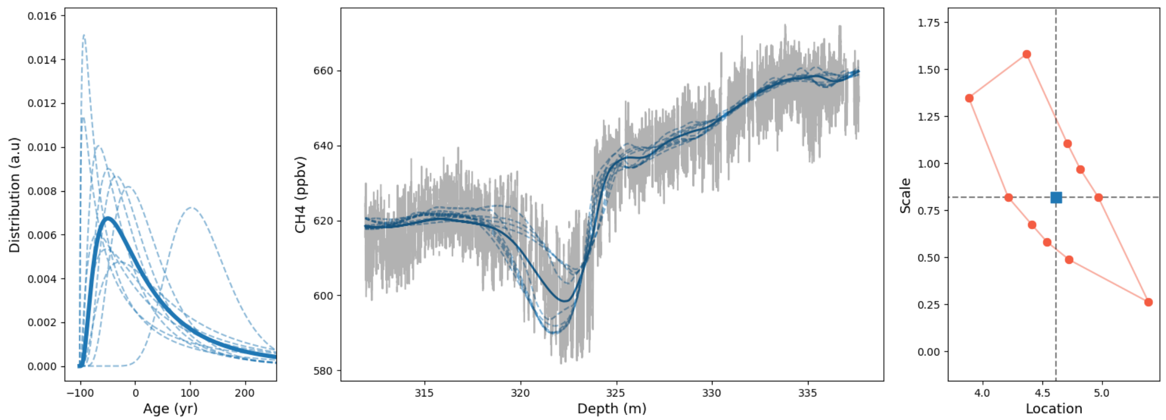

Figure S8. Same as Figure S3 for 8.2ka event in EDC99.

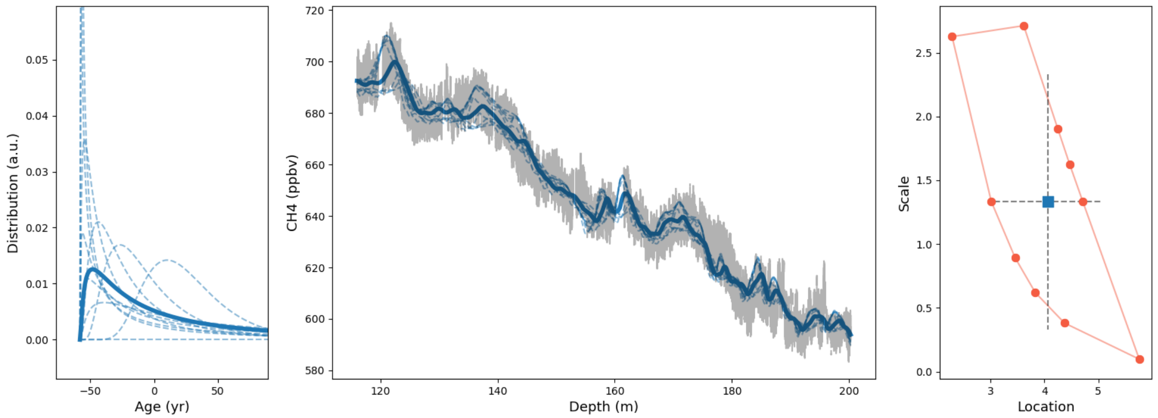

Figure S9. Same as Figure S3 for the modern section of Lock-In.

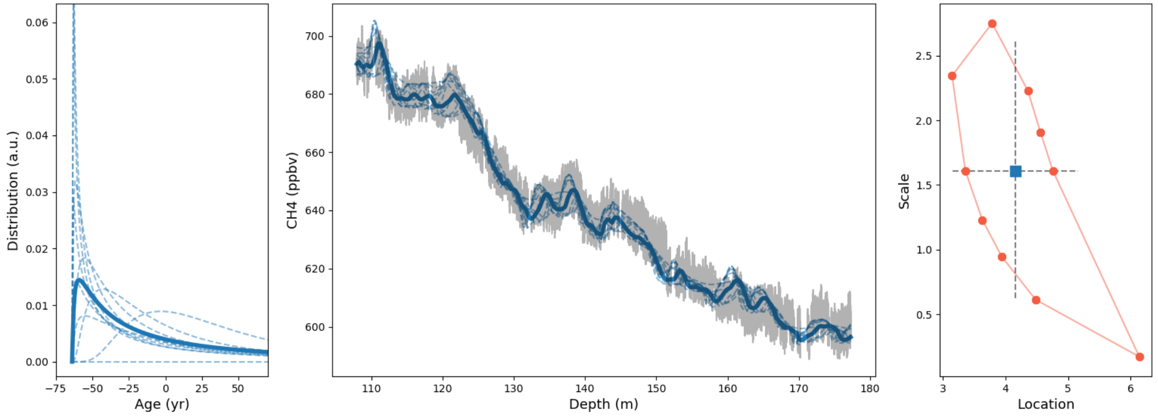

Figure S10. Same as Figure S3 for the modern section of Dome C.

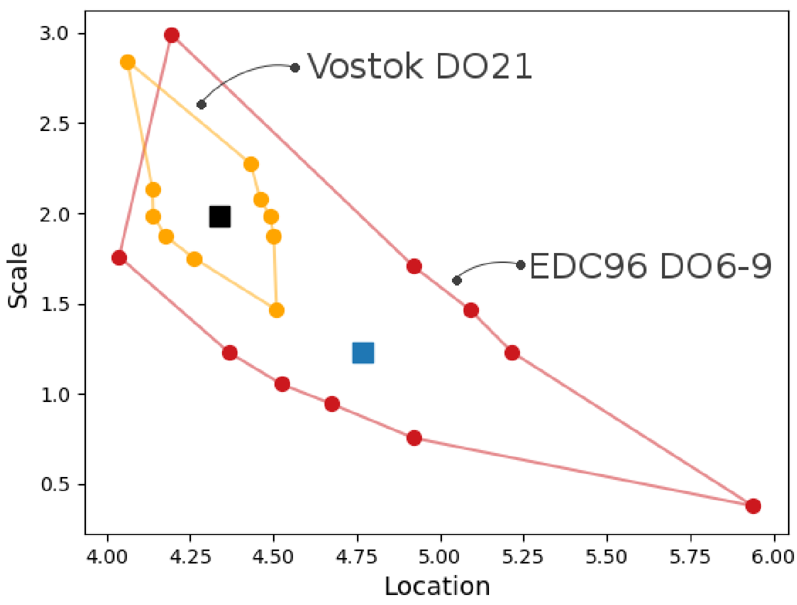

Figure S11. Uncertainty range of the location and scale parameters for the EDC96 DO6-8 and Vostok DO21 GADs. The EDC96 uncertainty range is represented as red dots, and the optimal EDC96 parameters is marked as a blue square. The Vostok DO21 uncertainty range is represented as orange dots, and the optimal Vostok DO21 parameters is marked as a black square.

References

Chappellaz, J., Stowasser, C., Blunier, T., Baslev-Clausen, D., Brook, E. J., Dallmayr, R., Faïn, X., Lee, J. E., Mitchell, L. E., Pascual, O., Romanini, D., Rosen, J., and Schüpbach, S.: High-resolution glacial and deglacial record of atmospheric methane by continuous-flow and laser spectrometer analysis along the NEEM ice core, Clim. Past, 9, 2579–2593, doi:10.5194/cp-9-2579-2013, 2013.

Fourteau, K., Faïn, X., Martinerie, P., Landais, A., Ekaykin, A. A., Lipenkov, V. Y., and Chappellaz, J.: Analytical constraints on layered gas trapping and smoothing of atmospheric variability in ice under low-accumulation conditions, Clim. Past, 13, 1815–1830, doi:10.5194/cp-13-1815-2017, 2017.

Loulergue, L., Schilt, A., Spahni, R., Masson-Delmotte, V., Blunier, T., Lemieux, B., Barnola, J.-M., Raynaud, D., Stocker, T. F., and Chappellaz, J.: Orbital and millennial-scale features of atmospheric CH_4 over the past 800,000 years, Nature, 453, 383–386, doi:10.1038/nature06950, 2008.